Ultra-Local Model-Based Intelligent Robust Control of PKMs: Theory and Simulations

Ghina Hassan, Ahmed Chemori, Maher El Rafei, Marc Gouttefarde, Clovis Francis, Pierre-Elie Hervé, Damien Sallé

14th IFAC International Workshop on
Adaptation and Learning in Control and Signal Processing
June 29 - July 1, 2022. Casablanca, Morocco

Ultra-Local Model-Based Intelligent Robust Control of PKMs: Theory and Simulations

G. Hassan [*,**] **A. Chemori** [*] **M. El Rafei** [**] **M. Gouttefarde** [*] **C. Francis** [**]
P.E. Hervé [***] **D. Sallé** [***]

[*] *LIRMM, Univ Montpellier, CNRS, Montpellier, France (e-mail: ghina.hassan, ahmed.chemori, marc.gouttefarde@lirmm.fr)*
[**] *CRSI, Lebanese University, Faculty of Engineering, Beirut, Lebanon (e-mail: maher.elrafei, cfrancis@ul.edu.lb)*
[***] *TECNALIA, Basque Research and Technology Alliance (BRTA), San Sebastian, Spain (e-mail: pierre-elie.herve, damien.salle@tecnalia.com)*

Abstract: In this paper, we propose a novel Intelligent Robust Control (IRC) suitable for controlling highly nonlinear Multiple-Input-Multiple-Output (MIMO) systems. The proposed IRC scheme takes advantage of the Robust Integral of the Sign of the Error (RISE) control law and Model-Free Control (MFC). The MFC scheme is mainly composed of: (i) a nonlinear function estimated from an ultra-local model representing the input-output behavior of the system, (ii) the v^{th} derivative of the reference trajectory as a feedforward term, and (iii) a feedback control term. MFC is characterized by its simple concept and its ability to compensate for the modeled and unmodeled system dynamics through its nonlinear compensation term. The proposed IRC approach consists of redesigning the feedback term of MFC scheme based on RISE feedback law to further improve its robustness against external disturbances and to guarantee a semi-global asymptotic tracking despite the presence of disturbances and uncertainties. Numerical simulations under different operating conditions have been conducted on T3KR parallel manipulator, in a pick-and-throw task, to validate the relevance of the proposed IRC strategy. The comparison with a model-based feedforward RISE and a feedforward super-twisting sliding mode control, by exploiting different performance indices, confirms the superiority of the proposed IRC approach.

Keywords: RISE feedback control, Model-Free Control, Intelligent Robust Control, Parallel Kinematic Manipulators, Pick-and-Throw, numerical simulations.

1. INTRODUCTION

Nowadays, most of industrial control systems are counted in the family of nonlinear MIMO systems. Indeed, these systems, known for their complex nonlinear dynamics, are often exposed to parameter variations and uncertainties, whether modeled or not, which makes their control design a challenging task. Therefore, adopting a conventional linear controller for such systems may deteriorate the tracking performance at critical operating conditions and even lead to instability in some situations. RISE is a robust nonlinear controller dedicated to the control of highly nonlinear MIMO systems. It was developed in (Xian et al., 2004) to ensure a semi-global asymptotic tracking of uncertain nonlinear systems under some assumptions on the controlled system. It is characterized by a unique feature which is the integral of the sign of the error, assuring its continuity as well as the rejection of external disturbances. Recently, the outstanding performance improvement brought by RISE and RISE-based controllers has been demonstrated on several nonlinear systems (Fischer et al., 2014; Yao et al., 2015; Kamaldin et al., 2016; Sherwani et al., 2020). The application of RISE control scheme on parallel kinematic manipulators (PKMs) was first proposed in (Bennehar et al., 2018), where a RISE-based adaptive controller was proposed and validated on a Delta parallel robot. Thanks to the good performance of this controller on PKMs, other research works have proposed other RISE-based control schemes for parallel robots. They include the time-varying RISE feedback control of (Saied et al., 2019), and the model-based feedforward RISE control of (Escorcia-Hernández et al., 2020). Recently, in (Hassan et al., 2020), the RISE feedback strategy has been applied, for the first time, on a cable-driven parallel robot (CDPR), showing a high positioning accuracy, despite the significant uncertainties inherent to such a system.

For several decades, model-based controllers have been considered as good candidates for the control of uncertain nonlinear systems. They have shown their ability to compensate for the system nonlinearities by introducing an apriori knowledge on the dynamic model in the control design. However, it is well known that the development of an accurate dynamic model for a complex nonlinear system is almost impossible. On one hand, unmodeled phenomena cannot be considered into such a model, and on the other hand, the system parameters are often subject to variations and uncertainties. Therefore, classical model-based controllers may lead to poor control performance of uncertain nonlinear systems, especially when changes in operating conditions occur or when the system parameters used in the control design do not match the actual parameters. To address this problem of parameters' variations and uncertainties, model-based adaptive controllers have been proposed in the literature. These control schemes include an adaptive feedforward term responsible for the online estimation of the un-

known, uncertain or time-varying dynamic parameters. Despite the simplicity of the principle of online parameters estimation, its real-time implementation requires a considerable number of calculations, which leads to a significant computing time. To deal with these issues, Fliess and Join proposed a MFC strategy to compensate for modeled and unmodeled dynamics as well as uncertainties, without incorporating any apriori knowledge about the physical system (Fliess, 2009). The MFC technique is based on an ultra-local model updated continuously in real-time based on the input-output behavior of the system. This numerical model is only valid for a small time lapse. The first MFC scheme was composed of an ultra-local model combined with a conventional Proportional-Integral-Derivative (PID) as a feedback control term. This control method is characterized by its simplicity and ease of implementation. Moreover, its design parameters can be adjusted in a straightforward manner. Model-free controllers have been widely used in recent years, showing a good tracking performance in various application fields. For instance, they have been applied to hydroelectric power plants (ROBERT and FLIESS, 2010), dc/dc converters (Michel et al., 2010), shape memory alloy active spring (Gédouin et al., 2009, 2011), underactuated mechanical systems (Andary and Chemori, 2011), active suspension systems of a quarter car (Wang et al., 2018), and recently to a PMSM drive system (Zhang et al., 2020).

Parallel robots are considered as second-order nonlinear uncertain MIMO systems, and are often subject to dynamic nonlinearities, parameters uncertainties, external disturbances, unmodeled phenomena, etc. Accordingly, several schemes have been proposed in the literature to accurately control PKMs. They include a linear feedback controller (Chaudhary and Ohri, 2016), a nonlinear control based on conventional PD (Su et al., 2004), robust controllers (Saied et al., 2019) (Castañeda et al., 2014), model-based control (Escorcia-Hernández et al., 2020), adaptive control (Natal et al., 2016). Although these controllers have shown good tracking performances, they remain suffering from a poor performance at critical operating conditions (e.g. high-precision and/or high-speed applications, payload changes). Indeed, some of them belong to the non-model-based control family, while the others are model-based controllers. On the one hand, the performance of non-model based controllers is limited to a small range of operations around the nominal steady state. Therefore, this class of controllers is not suitable for controlling PKMs, known for their complex nonlinear dynamics, and intended to be used in high-speed tasks. On the other hand, the issue with model-based controllers is that most nonlinear systems have uncertain and time-varying dynamic parameters and thereby very complex to be modeled. Thus, and as already mentioned, the system nonlinearities and its abundant uncertainties cannot be well compensated by adopting classical model-based control schemes. Even though adaptive controllers can overcome the drawbacks of model-based controllers by online estimating the parameters, their performance is limited to the compensation of modeled dynamics, while robustness against unmodeled ones cannot always be ensured.

In this paper, a novel IRC scheme is proposed. A revisit of the fundamental MFC scheme is carried out by redesigning its closed-loop feedback control term based on RISE feedback control law. Adopting the robust nonlinear RISE controller as a feedback term for the MFC can further improve its overall tracking performance and reinforce its robustness and disturbance rejection. For validation purposes, scenario-based numerical simulations are conducted in a Pick-and-Throw application using T3KR parallel robot. The proposed IRC scheme has been compared with two model-based robust controllers from the literature. The obtained simulation results show a significant improvement in the tracking performance and a more robustness towards disturbances and uncertainties.

The rest of this paper is structured as follows: A Background on MFC is provided in Section 2. Section 3 is dedicated to the proposed IRC strategy. The description and modeling of T3KR parallel robot are introduced in Section 4. Numerical simulation results are reported and discussed in Section 5. Conclusions and some future directions are provided in Section 6.

2. BACKGROUND ON MODEL-FREE CONTROL

Model-Free Control (MFC) is a strategy developed by Fliess (Fliess et al., 2006; Fliess, 2009) to control uncertain high-order nonlinear MIMO systems. It is said to be an "intelligent control", because it does not incorporate any knowledge about the system's dynamics, in the control design.

The basic principle of MFC is that the input-output behavior of a high-order nonlinear system, can be represented by an ultra-local model, continuously restructured, as follows:

$$y^{(\nu)} = F + \alpha U \tag{1}$$

where $\alpha \in \mathbb{R}^{n\times n}$ is positive-definite diagonal gain matrix, chosen by the designer to ensure some control performance. $y \in \mathbb{R}^n$ is the output vector, $U \in \mathbb{R}^n$ is the control input vector and $F \in \mathbb{R}^n$ is a vector gathering the modeled and unmodeled system dynamics. $\nu \in \mathbb{N}$ denotes the order of the anticipated model.

F can be estimated at each sampling time from the measured output y, and the known input U, as follows (Fliess and Join, 2013):

$$[F(k)]_e = [y^{(\nu)}(k)]_e - \alpha U(k-1) \tag{2}$$

where $[F(k)]_e$ is the estimation at the sample k of the function F (i.e. $t = kT_s$ is the sampling time with $k = 0, 1, \ldots$ and T_s is the sampling period), $[y^{(\nu)}(k)]_e$ denotes the estimation of the ν-derivative of y at time k, and $U(k-1)$ is the control input at the previous sample time. It is worth to note that this estimation is only valid for a short interval of time, and should be updated frequently and continuously to maintain the system stability with a good tracking performance.

In general, the model-free control input U is computed at each iteration, based on the following expression:

$$U(k) = -\frac{[F(k)]_e}{\alpha} + \frac{y_d^{(\nu)}(k) + U_c(k)}{\alpha} \tag{3}$$

where $y_d^{(\nu)}$ is the ν^{th} derivative of the desired trajectory, and U_c is the feedback control law that should be selected in a way to guarantee asymptotic convergence of the output signal to the desired trajectory.

The designer must choose the value of the order ν, carefully, taking into account the order of the controlled system and the structure of the feedback control input. Otherwise, the stability of the system may be deteriorated. In general, ν can be chosen to be 1 or 2. For instance, intelligent PID (iPID) is designed with $\nu = 2$, while intelligent PI (iPI) is used with $\nu = 1$.

In practice, the measured output is often subject to noise, which may be amplified by the numerical derivative. Regarding this issue, some methods have been proposed in the literature to compute the ν^{th} derivative of noisy signals using an algebraic approach. The differential algebraic operations are composed of iterated integrals of the noisy signal taking the form of classical

finite impulse response (FIR) digital filters (Fliess and Join, 2013; Mboup et al., 2009; Gédouin et al., 2011); while other methods have approximated the value of F by exploiting an extended state observer (Wang et al., 2018; Zhang et al., 2020).

3. PROPOSED CONTRIBUTION: INTELLIGENT ROBUST CONTROL

3.1 Background on RISE feedback control

As stated in (Xian et al., 2004), RISE is a robust continuous control scheme developed for high-order MIMO nonlinear systems. It is a full-state feedback non-mode-based control scheme. In addition, RISE can ensure semi-global asymptotic tracking under some assumptions on the system and the reference trajectory.
Consider the dynamic equation of a second-order MIMO nonlinear system as follows:

$$M(x,\dot{x})\ddot{x}+F(x,\dot{x})=U \tag{4}$$

where x, $\dot{x}$ and $\ddot{x}\in\mathbb{R}^n$ are the position, velocity and acceleration states of the system, respectively. $M(x,\dot{x})\in\mathbb{R}^{n\times n}$ and $F(x,\dot{x})\in\mathbb{R}^n$ being uncertain nonlinear functions, $U\in\mathbb{R}^n$ is the control input vector, and n is the actuators number. The assumptions, considered in (Xian et al., 2004), are as follows:
Assumption 1: *$M(x,\dot{x})$ is a symmetric positive-definite matrix that satisfies the following inequalities for any $\gamma\in\mathbb{R}^n$:*

$$\underline{m}\|\gamma\|^2\leq\gamma^T M(x,\dot{x})\gamma\leq\bar{m}(x)\|\gamma\|^2 \tag{5}$$

where $\underline{m}$ is a known positive constant and $\bar{m}(x)$ is a positive non-decreasing function.
Assumption 2: *$F(x,\dot{x})$ is bounded if x and $\dot{x}$ are measurable and bounded. Moreover, $M(x,\dot{x})$ and $F(x,\dot{x})$ are second-order differentiable with respect to $x(t)$ and $\dot{x}(t)$.*
Assumption 3: *The chosen desired trajectory $x_d(t)\in\mathbb{R}^n$ is continuously differentiable with respect to time up to the 4^{th} order. $x_d(t)$ and its derivatives $\in\mathscr{L}_\infty$.*
Let us now define the combined tracking error $e_2\in\mathbb{R}^n$ as follows:

$$e_2=\dot{e}_1+\lambda e_1. \tag{6}$$

where $e_1=x_d-x$, is the output tracking error, while x_d and $x\in\mathbb{R}^n$ are the reference trajectory and the measured one, respectively. $\lambda\in\mathbb{R}^{n\times n}$ is a positive-definite, diagonal gain matrix.

Based on the stability analysis, detailed in (Xian et al., 2004), the RISE feedback control law is expressed as follows:

$$\begin{aligned}U(t)&=(K_s+I)e_2(t)-(K_s+I)e_2(t_0)\\&+\int_{t_0}^{t}[(K_s+I)\Lambda e_2(\sigma)+\beta sgn(e_2(\sigma))]d\sigma.\end{aligned} \tag{7}$$

where K_s and $\beta\in\mathbb{R}^{n\times n}$ are two diagonal positive-definite control design matrices, $I\in\mathbb{R}^{n\times n}$ is the identity matrix, t_0 is the initial time and $sgn(.)$ represents the standard signum function. The integral of signum constitutes the robustness term of the RISE control law thanks to which smooth bounded disturbances can be held. It is worth to note that the second term of the R.H.S of (7) (i.e., $(K_s+I)e_2(t_0)$) is introduced to guarantee a zero control input at time $t=t_0$ (i.e., $U(t_0)=0$). The stability of the RISE feedback law has been proved in (Xian et al., 2004), for large enough values of the gains K_s, λ, Λ and for a sufficient condition on β. It shows that all the system signals are bounded and converge to zero as time goes to infinity, i.e. $e_1^{(i)}=0$ as $t\to\infty$, for $i=0,1,2$ (the reader can refer to (Xian et al., 2004) for more details about the stability analysis of RISE feedback control).

3.2 Proposed intelligent robust control

As presented in the previous section, RISE is a non-model-based controller. This means that the system nonlinearities and uncertainties are not well compensated by such a controller, resulting in a degraded tracking performance in critical situations (e.g. high-speed movements, and in the presence of large disturbances). As stated in the introduction, the extension of this controller with a classical model-based feedforward term is not an effective idea since it is almost impossible to obtain an accurate dynamic model of a complex nonlinear system. This issue becomes considerable in industrial Pick-and-Place or Pick-and-Throw (Raptopoulos et al., 2020) applications, where the robot should handle different types of objects with unknown/uncertain dynamic parameters. The aforementioned MFC scheme has the ability to compensate for parameter variations, modeled and unmodeled dynamics without considering any knowledge of the system dynamics in the control design. However, the feedback control term of the fundamental MFC consists of a conventional linear PID which may lead to poor performance when dealing with a highly nonlinear system, especially at high accelerations. In this work, we propose to revise the conventional MFC scheme known as iPID by redesigning its feedback control term based on the RISE feedback law. This revision can significantly improve the tracking performance of MFC as well as its robustness towards external disturbances, while preserving the simplicity of its scheme. The resulting controller, called Intelligent Robust Control (IRC), is continuous, robust and easy to implement. The proposed IRC strategy for second-order MIMO systems can be expressed as follows:

$$\Gamma_{IRC}=-\frac{[F]_e}{\alpha}+\frac{\ddot{x}_d+\Gamma_{RISE}}{\alpha} \tag{8}$$

where Γ_{RISE} is the RISE feedback law presented in (7). As reported in (Gédouin et al., 2011), if the order of the controlled system is well known, then the ν order of the numerical model as given in equation (3) will be equal to that of the system. Therefore, in our case, for a system of second order as PKMs, ν is equal to 2.

4. APPLICATION TO T3KR PARALLEL ROBOT

4.1 T3KR robot: description and kinematics

The T3KR robot is a 5-DOF PKM, developed in collaboration between Tecnalia, LIRMM and SATT AxLR. It was proposed as a new industrial "Pick-and-Place" machine with the possible economic footprint (i.e. it has an optimized mechanical structure). Fig. 1 illustrates, through a CAD-view, the robot T3KR as well as its main components. It consists of a fixed-base support holding four main actuators and connected to a common moving platform through four kinematic chains. Each chain consists of a serial connection of a rotary servo actuator, a rear arm that is supposed to rotate, and a forearm consisting of two parallel bars. The forearms are mounted, from their first extremity, to the rear arms, and from their other extremity, to the mobile platform by means of passive spherical joints. Besides, this robot includes an actuator fixed on the mobile platform allowing a rotation ϕ of the end-effector around the vertical z-axis. The parallel structure with the four motors allows the

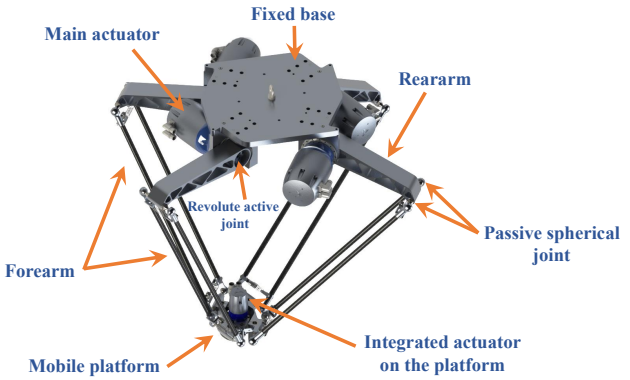

Fig. 1. A CAD View of T3KR robot and its main components.

translation of the platform along x, y and z axes as well as its rotation ψ around the z-axis, which is kinematically redundant; the rotation of the platform is a parallelogram mechanism movement, where the tool control point (TCP) is on the neutral point of this mechanism. Accordingly, a rotation ψ of the moving platform does not induce a motion of the TCP, this is why ψ is kept equal to zero.
In this study, we are interested in controlling the main four actuators of the parallel Delta-like positioning structure to do a pick-and-throw task. Thus, the Cartesian vector representing the pose of the end-effector of the robot is a 4-dimensional coordinate denoted by $X = [x, y, z, \psi]^T$. The vector representing the actuated joint positions is a 4-dimensional coordinate vector given by $q = [q_1, q_2, q_3, q_4]^T$. The differential kinematic relationship between the Cartesian and joint velocities can be expressed as $\dot{X} = J\dot{q}$, where $\dot{X}$ and $\dot{q}$ are the Cartesian and joint velocities, respectively and J is the direct Jacobian matrix.

4.2 T3KR robot dynamics

As T3KR is a Delta-like parallel robot, its dynamic model can be developed by adopting the virtual work principle (Codourey, 1998; Bennehar et al., 2018), while considering some simplification assumptions. The dynamics of T3KR robot can be reduced to the analysis of the dynamics of the moving platform and those of the actuators with their corresponding rear arms and forearms. From the moving platform side, one can define two kinds of forces: the gravitational force and the force induced by the Cartesian acceleration. The contributions of these two forces at the level of actuators can be obtained by using the transpose of the Jacobian matrix J. From the actuators side, we have the input torques generated by the motors, the gravitational forces of the rear arms and the inertial torques resulting from the rear arms rotation.
Following the same analysis as in (Codourey, 1998), the inverse dynamic equation of T3KR parallel robot can be expressed in joint space as follows:

$$M(q)\ddot{q} + C(q,\dot{q})\dot{q} + G(q) + D(q,\dot{q},t) = \Gamma(t) \tag{9}$$

where $q, \dot{q}, \ddot{q} \in \mathbb{R}^4$ are vectors of the joint positions, velocities, and accelerations, respectively, $M(q) \in \mathbb{R}^{4\times4}$ is the total mass and inertia matrix of the robot, $C(q,\dot{q}) \in \mathbb{R}^{4\times4}$ is the Coriolis and centrifugal forces matrix, $G(q) \in \mathbb{R}^4$ is the gravitational forces vector acting on the rear arms and the moving platform, $D(q,\dot{q},t) \in \mathbb{R}^4$ is the vector of the disturbances (i.e. unmodeled dynamics, external disturbances, etc.). $\Gamma(t) \in \mathbb{R}^4$ is the vector of the control input torques.

Table 1. Summary of the main kinematic and dynamic parameters of T3KR parallel robot.

Parameter	Value	Parameter	Value
Rear arm length	400 mm	Traveling plate mass	5.68 kg
Forearm length	900 mm	Actuator inertia	0.000969 kg.m^2
Rear arm mass	3.28 kg	Rear arm inertia	0.173723 kg.m^2
Forearm mass	0.8 kg		

The main kinematic and dynamic parameters of T3KR parallel robot are summarized in Table 1.

4.3 Control application on T3KR robot

To demonstrate the relevance of the proposed IRC, a comparative study between the proposed control scheme and other control methods recently proposed in literature, has been performed. The obtained numerical simulation results, on the T3KR parallel robot, are presented and discussed in the next section. The T3KR PKM is a second-order MIMO nonlinear system with four control signals as inputs and four joint positions as outputs. Its complex nonlinear dynamic model can be approximated using an ultra-local model.
To properly represent the dynamics of T3KR, the ultra-local model in (1) can be redefined as follows:

$$\ddot{q} = F + \alpha U \tag{10}$$

where, $F \in \mathbb{R}^4$, $\mathrm{U} \in \mathbb{R}^4$ and $\alpha \in \mathbb{R}^{4\times4}$. While ν is equal to 2 as our controlled system is a second order MIMO system.

One can note that the dynamics (9) of T3KR robot is considered as a particular case of the nonlinear system presented in (4) with $n = 4$ and can rewritten as follows:

$$A(.)\ddot{q} + B(.) = \Gamma \tag{11}$$

where $A(.) = M(q)$ and $B(.) = C(q,\dot{q})\dot{q} + G(q) + D(q,\dot{q},t)$. As a consequence, $M(q)$ is a positive definite symmetric matrix satisfying Assumption 1. Assumption 2 is also satisfied such that the signals $q(t)$ and $\dot{q}(t)$ are measurable and bounded, resulting in $B(.)$ being bounded. Moreover, the matrices $M(q)$, $C(q,\dot{q})$, $G(q)$ and $D(q,\dot{q},t)$ are differentiable to second order with respect to $q(t)$ and $\dot{q}(t)$. And finally, the chosen reference trajectory $q_d(t)$ is designed to be continuously differentiable, as reported in Assumption 3.
The dynamics of T3KR robot fits the design of the proposed IRC scheme. Therefore, it is possible to apply the IRC strategy to the T3KR robot. For proper implementation of controllers, the tracking error e_1 needs to be redefined as: $e_1 = q_d - q$, where $q_d \in \mathbb{R}^4$ is the vector of the desired joint positions and $q \in \mathbb{R}^4$ is the vector of the measured joint positions.

5. NUMERICAL SIMULATION RESULTS

5.1 State-of-the-art control methods for comparison purposes

The model-based feedforward RISE control (FF-RISE) developed in (Escorcia-Hernández et al., 2020), and the model-based feedforward super-twisting sliding mode control (FF-ST-SMC) proposed in (Saied et al., 2021) for the control of PKMs, are also implemented for comparison purposes, since they are both model-based robust controllers. Their control laws are given as follows:

$$\begin{aligned}\Gamma_{FF-RISE} = {} & M(q_d)\ddot{q}_d + C(q_d,\dot{q}_d)\dot{q}_d + G(q_d) \\ & + (K_s + I)e_2(t) - (K_s + I)e_2(t_0) \\ & + \int_{t_0}^{t} [(K_s + I)\Lambda e_2(\sigma) + \beta sgn(e_2(\sigma))]d\sigma.\end{aligned} \tag{12}$$

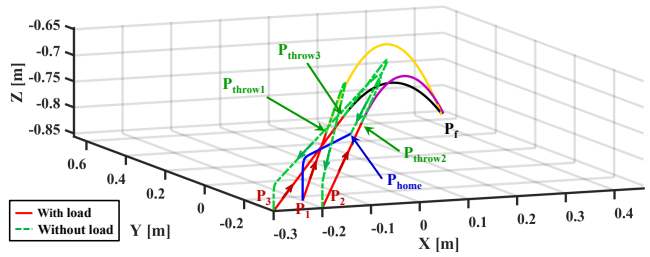

Fig. 2. 3D-view of the P&T reference trajectory.

$$\Gamma_{FF-ST-SMC} = M(q_d)\ddot{q}_d + C(q_d,\dot{q}_d)\dot{q}_d + G(q_d) + K_1 s + K_2|s|^{1/2}sgn(s) + \int K_3\, sgn(s). \quad (13)$$

where s is the standard sliding surface defined as $s = \dot{e}_1 + \lambda e_1$. K_1, K_2, and K_3 are three positive definite diagonal gain matrices, and λ is a positive constant gain.

5.2 Pick-and-Throw reference trajectory

The P&T trajectory, illustrated in Fig. 2, is used for the validation of the proposed control scheme. It is generated in Cartesian space using a third order polynomial S-curve as a motion profile. The generated trajectory corresponds to the scenario of three objects of different masses thrown successively into a target position, $\mathbf{P}_f$, located outside the workspace of the robot. The first movement of the robot's end-effector is from its central position $\mathbf{P}_{home}$ towards the first pick position, $\mathbf{P}_1$, to grasp the first object. According to the pick and target positions of the corresponding object, an appropriate release position $\mathbf{P}_{throw_1}$ is computed. Next, the robot accelerates to this position, and then it throws the object into the desired target $\mathbf{P}_f$. After releasing the object, the robot decelerates back to pick the next object, while the thrown object follows its ballistic trajectory from $\mathbf{P}_{throw_1}$ to $\mathbf{P}_f$. The same scenario is repeated for the second and the third objects, located at $\mathbf{P}_2$ and $\mathbf{P}_3$, respectively. Once the third object is thrown, the robot returns back its home position $\mathbf{P}_{home}$. The whole trajectory is generated taking into account the physical limits of the robot (i.e. maximum jerk, acceleration and velocity), its workspace and the desired target position. The sections of the trajectory where the moving platform is carrying the object are depicted with solid red lines, whereas the dashed green lines correspond to the sections of the trajectory after the release point where the robot is moving without any payload (cf. Fig. 2).

5.3 Performance evaluation criteria

The most commonly used performance index for the evaluation of the tracking performance of new control algorithms is the Root Mean Square Error (*RMSE*) criterion. It is adopted in this study for Cartesian translational positions tracking $RMSE_x$ as well as joint positions tracking $RMSE_J$ as follows:

$$RMSE_x = \sqrt{\left(\frac{1}{N}\sum_{i=1}^{N}(e_x^2(i) + e_y^2(i) + e_z^2(i))\right)} \quad (14)$$

$$RMSE_J = \sqrt{\left(\frac{1}{N}\sum_{i=1}^{N}(e_{q_1}^2(i) + e_{q_2}^2(i) + e_{q_3}^2(i) + e_{q_4}^2(i))\right)} \quad (15)$$

with e_x, e_y and e_z denote the Cartesian position tracking errors along the three translational axes, x, y and z. e_{q_1}, e_{q_2}, e_{q_3} and e_{q_4} are the joint position tracking errors. N is the total number of samples.

Table 2. Summary of the feedback control gains.

FF-RISE		FF-ST-SMC		Proposed IRC	
$\lambda = 150$	$\beta = 2.5$	$K_1 = 18.2$	$\lambda = 200$	$\lambda = 150$	$\beta = 2.5$
$\Lambda = 0.3$		$K_2 = 0.23$		$\Lambda = 0.3$	$\alpha = 1.6$
$K_s = 22$		$K_3 = 2.5$		$K_s = 22$	

5.4 Tuning of the control gains

For tuning the gains of all implemented controllers, we adopted the trial-and-error method. The gains of the proposed IRC strategy can be adjusted using the following procedure: (i) first, set the values of α and λ large enough to have an acceptable steady-state error. Then (ii) decrease the value of α until getting a quick oscillatory response of the output. (iii) Modify λ and K_s to stabilize the system with a satisfactory tracking performance. (iv) Increase Λ, and at the same time, adjust λ and K_s up or down until the best performance index is achieved. (v) The robustness of the controller may be improved by increasing the feedback gain β gradually to avoid chattering in the control signals. The obtained control gains for all controllers are summarized in Table 2.

5.5 Numerical simulations results

In order to evaluate the performance of the proposed intelligent robust controller, a comparative study has been performed with the aforementioned feedforward RISE and feedforward ST-SMC controllers through numerical simulations in Matlab/Simulink environment. The reference P&T trajectory, plotted in Fig.2, has been considered for this study. Two main scenarios have been implemented on the T3KR robot: 1) Scenario 1: robustness towards payload changes, 2) Scenario 2: robustness towards velocity variations. For more realistic simulations, white noise has been added to the output joint positions (this noise acts as the measurement noise affecting the real joint positions) as well as a 25% of uncertainty on the inertia value including the inertia of the actuators, the inertia of the rear arms and the inertial contribution of the forearms has been considered.

Scenario 1 - Robustness towards payload changes: In this scenario, the maximum operating acceleration was set to 4.2 G, which is the minimum value sufficient to throw an object outside the robot workspace. The three objects, used for this validation, have different masses: the first one has a mass of 50 g, the second one has a mass of 100 g (i.e. $\Delta_{mass} = +100\,\%$ w.r.t the first object), while the third one has a mass of 150 g (i.e. $\Delta_{mass} = +200\,\%$ w.r.t the first object). Therefore, the robustness of the proposed controller towards payload changes can be demonstrated using this scenario.
The Cartesian tracking errors of the three controllers are depicted in Fig. 3. The obtained results show that the contribution of the ultra-local model improves the performance of the conventional FF-RISE controller by 54.7% and 61.1% for the Cartesian and joint spaces, respectively (see Table 3). Compared to the FF-ST-SMC strategy, the proposed IRC improves the tracking performance by up to 33.7% and 41.6% in the Cartesian and joint spaces, respectively.
Fig. 4 represents the evolution of the control input torques generated by all controllers, and clearly shows that the control signals are below the saturation limits of the actuators (the maximum torque of T3KR actuators is 28.9 N.m). Moreover, we

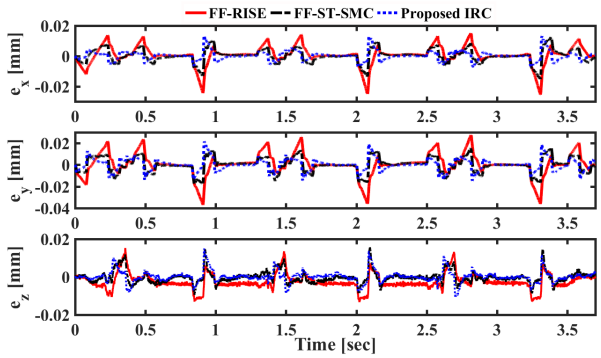

Fig. 3. Scenario 1: Evolution of the Cartesian tracking errors.

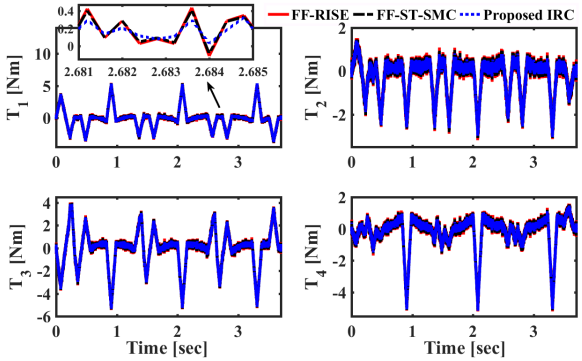

Fig. 4. Scenario 1: Evolution of the control input torques.

can notice from Fig. 4 that the proposed IRC strategy slightly reduces the power consumption since it generates less input torques, compared to FF-RISE and FF-ST-SMC schemes.
This scenario confirms the improvement achieved by considering an ultra-local model, updated in real time, instead of a conventional feedforward dynamic model. According to the evaluation criteria, reported in Table 3, the proposed IRC algorithm shows higher accuracy and better robustness to payload variations than the two other model-based controllers; this is highly relevant for P&T sorting applications where the robot has to deal with different types of objects.

Scenario 2 - Robustness towards speed variations: The T3KR robot is intended to be used for high-speed P&T sorting applications. For this purpose, it is important to evaluate the tracking performance of the proposed IRC algorithm for high accelerations. The operating speed is increased to an acceleration of 9 G while performing the same P&T trajectory with the same manipulated objects as the previous scenario.
In Fig. 5, we can see the relevant improvements obtained by the proposed control scheme along all translation axes. These improvements are quantified by exploiting the RMSE evaluation criteria in Cartesian and joint spaces. The obtained results, summarized in Table 3, show improvements of 51.7% in the Cartesian space and 60.4% in the joint space relative to the FF-RISE controller. In comparison to the FF-ST-SMC scheme, the tracking performance is improved by up to 41.6% and 52.5% in the Cartesian and joint spaces, respectively.
The evolution of the control input signals, generated by the three implemented controllers, are displayed in Fig. 6. Indeed, it is obvious that all the control signals evolve within the admissible range of the actuators' capabilities. As it can be seen from Fig. 4, a slight reduction in energy consumption is notified for the proposed controller compared to the two other controllers.

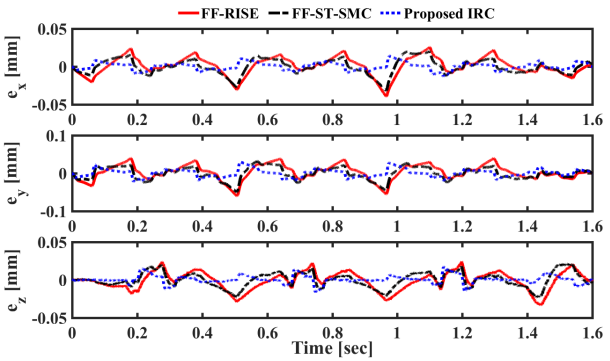

Fig. 5. Scenario 2: Evolution of the Cartesian tracking errors.

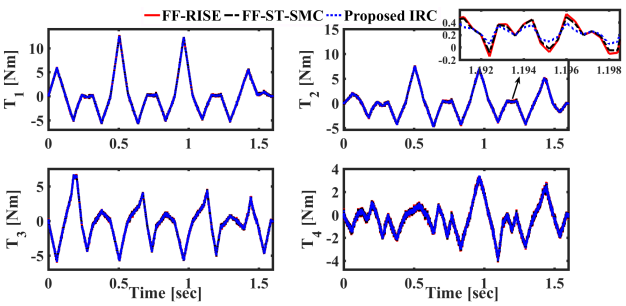

Fig. 6. Scenario 2: Evolution of the control input torques.

The overall performance improvement, obtained by the proposed IRC scheme, can be explained by the good compensation of the system nonlinearities provided by the contribution of the ultra-local model with the RISE feedback law.

Table 3. Control performance evaluation

Scenario	Control	$RMSE_X$[mm]	$RMSE_J$[deg]
Scenario 1	FF-RISE	0.0126	0.0018
	FF-ST-SMC	0.0086	0.0012
	Proposed IRC	0.0057	0.0007
	IMP w.r.t FF-RISE	**54.7 %**	**61.1 %**
	IMP w.r.t FF-ST-SMC	**33.7 %**	**41.6 %**
Scenario 2	FF-RISE	0.0259	0.0048
	FF-ST-SMC	0.0214	0.0040
	Proposed IRC	0.0125	0.0019
	IMP w.r.t FF-RISE	**51.7 %**	**60.4 %**
	IMP w.r.t FF-ST-SMC	**41.6 %**	**52.5 %**

6. CONCLUSION AND FUTURE WORK

In this paper, an Intelligent Robust Controller (IRC), dedicated to high-order nonlinear MIMO systems, has been proposed. It is a new design of the MFC scheme consisting of exploiting the RISE feedback law in its feedback control term. RISE is a robust control law that can further empower the MFC with more robustness against disturbances and improve its overall tracking performance. The proposed IRC technique can compensate for modeled and unmodeled dynamics without requiring any apriori knowledge about the controlled system. It has been implemented, through numerical simulations, on T3KR parallel robot in a Pick-and-Throw application under different operating conditions. The obtained results show clearly that the proposed control scheme outperforms both the feedforward RISE and feedforward ST-SMC controllers. However, the proposed control method presents some limitations. For instance, the gain parameter α, if not well chosen, will lead to actuators

saturation and thus performance deterioration. Moreover, this controller depends on the estimation of the real acceleration from the measured positions. Although different methods have been proposed in the literature for the estimation of noisy signals, the issue remains open. This work can be extended by the stability analysis of the resulting closed-loop system as well as by its implementation in real-time experiments. In addition, nonlinear or adaptive gains depending on the system state errors can be adopted in the feedback control term of the proposed MFC scheme instead of static gains. The time-varying gains can produce corrective control actions ensuring the establishment of the desired performance.

ACKNOWLEDGEMENTS

This work is supported by Tecnalia "Pick-and-Throw" research project. The corresponding author acknowledged the Lebanese University and the social foundation AZM and SAADE for financial support.

REFERENCES

Andary, S. and Chemori, A. (2011). A dual model-free control of non-minimum phase systems for generation of stable limit cycles. In *2011 50th IEEE Conference on Decision and Control and European Control Conference*, 1387–1392. IEEE.

Bennehar, M., Chemori, A., Bouri, M., Jenni, L.F., and Pierrot, F. (2018). A new rise-based adaptive control of pkms: design, stability analysis and experiments. *International Journal of Control*, 91(3), 593–607.

Castañeda, L.A., Luviano-Juárez, A., and Chairez, I. (2014). Robust trajectory tracking of a delta robot through adaptive active disturbance rejection control. *IEEE Transactions on control systems technology*, 23(4), 1387–1398.

Chaudhary, G. and Ohri, J. (2016). 3-dof parallel manipulator control using pid controller. In *2016 IEEE 1st International Conference on Power Electronics, Intelligent Control and Energy Systems (ICPEICES)*, 1–6. IEEE.

Codourey, A. (1998). Dynamic modeling of parallel robots for computed-torque control implementation. *The International Journal of Robotics Research*, 17(12), 1325–1336.

Escorcia-Hernández, J.M., Chemori, A., Aguilar-Sierra, H., and Monroy-Anieva, J.A. (2020). A new solution for machining with ra-pkms: Modelling, control and experiments. *Mechanism and Machine Theory*, 150, 103864.

Fischer, N., Hughes, D., Walters, P., Schwartz, E.M., and Dixon, W.E. (2014). Nonlinear rise-based control of an autonomous underwater vehicle. *IEEE Transactions on Robotics*, 30(4), 845–852.

Fliess, M. (2009). Model-free control and intelligent pid controllers: towards a possible trivialization of nonlinear control? *IFAC Proceedings Volumes*, 42(10), 1531–1550.

Fliess, M. and Join, C. (2013). Model-free control. *International Journal of Control*, 86(12), 2228–2252.

Fliess, M., Join, C., Mboup, M., and Sira-Ramirez, H. (2006). Vers une commande multivariable sans modèle. *arXiv preprint math/0603155*.

Gédouin, P.A., Delaleau, E., Bourgeot, J.M., Join, C., Chirani, S.A., and Calloch, S. (2011). Experimental comparison of classical pid and model-free control: position control of a shape memory alloy active spring. *Control Engineering Practice*, 19(5), 433–441.

Gédouin, P.A., Join, C., Delaleau, E., Bourgeot, J.M., Arbab-Chirani, S., and Calloch, S. (2009). A new control strategy for shape memory alloys actuators. In *8th European Symposium on Martensitic Transformations*, CDROM.

Hassan, G., Chemori, A., Chikh, L., Hervé, P.E., El Rafei, M., Francis, C., and Pierrot, F. (2020). Rise feedback control of cable-driven parallel robots: design and real-time experiments. *IFAC-PapersOnLine*, 53(2), 8519–8524.

Kamaldin, N., Chen, S.L., Kong, C.J., Teo, C.S., and Tan, K.K. (2016). Adaptive parameter and gain rise control of a flexure-based dual-drive 'h'gantry. In *2016 IEEE International Conference on Advanced Intelligent Mechatronics (AIM)*, 1240–1245. IEEE.

Mboup, M., Join, C., and Fliess, M. (2009). Numerical differentiation with annihilators in noisy environment. *Numerical algorithms*, 50(4), 439–467.

Michel, L., Join, C., Fliess, M., Sicard, P., and Chériti, A. (2010). Model-free control of dc/dc converters. In *2010 IEEE 12th workshop on control and modeling for power electronics (COMPEL)*, 1–8. IEEE.

Natal, G.S., Chemori, A., and Pierrot, F. (2016). Nonlinear control of parallel manipulators for very high accelerations without velocity measurement: stability analysis and experiments on par2 parallel manipulator. *Robotica*, 34(01), 43–70.

Raptopoulos, F., Koskinopoulou, M., and Maniadakis, M. (2020). Robotic pick-and-toss facilitates urban waste sorting. In *2020 IEEE 16th International Conference on Automation Science and Engineering (CASE)*, 1149–1154. IEEE.

ROBERT, G. and FLIESS, M. (2010). Model-free based water level control for hydroelectric power plants. *IFAC Proceedings Volumes*, 43(1), 134–139.

Saied, H., Chemori, A., Bouri, M., El Rafei, M., Francis, C., and Pierrot, F. (2019). A new time-varying feedback rise control for second-order nonlinear mimo systems: theory and experiments. *International Journal of Control*, 1–14.

Saied, H., Chemori, A., El Rafei, M., and Francis, C. (2021). A novel model-based robust super-twisting sliding mode control of pkms: Design and real-time experiments. In *IEEE/RSJ International Conference on Intelligent Robots and Systems (IROS 2021)*.

Sherwani, K.I., Kumar, N., Chemori, A., Khan, M., and Mohammed, S. (2020). Rise-based adaptive control for eicosi exoskeleton to assist knee joint mobility. *Robotics and Autonomous Systems*, 124, 103354.

Su, Y., Duan, B., and Zheng, C. (2004). Nonlinear pid control of a six-dof parallel manipulator. *IEE Proceedings-Control Theory and Applications*, 151(1), 95–102.

Wang, H., Mustafa, G.I., and Tian, Y. (2018). Model-free fractional-order sliding mode control for an active vehicle suspension system. *Advances in Engineering Software*, 115, 452–461.

Xian, B., Dawson, D.M., de Queiroz, M.S., and Chen, J. (2004). A continuous asymptotic tracking control strategy for uncertain nonlinear systems. *IEEE Transactions on Automatic Control*, 49(7), 1206–1211.

Yao, J., Deng, W., and Jiao, Z. (2015). Rise-based adaptive control of hydraulic systems with asymptotic tracking. *IEEE Transactions on Automation Science and Engineering*, 14(3), 1524–1531.

Zhang, Y., Jin, J., and Huang, L. (2020). Model-free predictive current control of pmsm drives based on extended state observer using ultralocal model. *IEEE Transactions on Industrial Electronics*, 68(2), 993–1003.